Correlation between stress and hardness in pulsed cathodic arc deposited titanium/vanadium nitride alloys

2004 J. Phys.: Condens. Matter 16 7947

(http://iopscience.iop.org/0953-8984/16/45/017)

INSTITUTE OF PHYSICS PUBLISHING JOURNAL OF PHYSICS: CONDENSED MATTER

J. Phys.: Condens. Matter **16** (2004) 7947–7954 PII: S0953-8984(04)82482-2

Correlation between stress and hardness in pulsed cathodic arc deposited titanium/vanadium nitride alloys

K E Davies[1,4], B K Gan[1], D R McKenzie[1], M M M Bilek[1], M B Taylor[2], D G McCulloch[2] and B A Latella[3]

[1] School of Physics, University of Sydney, NSW 2006, Australia
[2] Applied Physics, School of Applied Sciences, RMIT University, GPO Box 2476V, Melbourne, 3001, Australia
[3] Materials and Engineering Science, Australian Nuclear Science and Technology Organisation, Private Mail Bag 1, Menai, NSW 2234, Australia

E-mail: kerrie@physics.usyd.edu.au (K E Davies)

Received 22 June 2004, in final form 14 October 2004
Published 29 October 2004
Online at stacks.iop.org/JPhysCM/16/7947
doi:10.1088/0953-8984/16/45/017

Abstract

We use a dual source pulsed cathodic arc with centre triggering to produce alloys in the series $Ti_{1-x}V_xN$ with accurately controlled composition. We show that the composition $x = 0.23$ produces the highest indentation hardness and hence the highest yield stress. This composition also shows the highest stress levels, which we explain in terms of its reduced flow during deposition. The microstructure of the alloys shows that they are homogeneously mixed with the rocksalt structure. At the highest vanadium contents a (200) preferred orientation develops. This work shows that the composition $Ti_{0.77}V_{0.23}N$ has a substantially higher hardness than TiN and may have an application as a high performance alloy.

1. Introduction

Many of the transition metals form nitrides which can be prepared as thin film coatings with high hardness and high wear resistance. Alloying of the transition metal nitrides offers the possibility of producing even higher hardness and of extending the range of colours available in high performance coatings. Here we investigate the alloys of titanium nitride (TiN) and vanadium nitride (VN) in order to assess their potential for this purpose. TiN and VN have the same face centred cubic (rocksalt) structure, similar lattice parameters [1] and are miscible over the complete composition range [2]. The properties are therefore expected to vary continuously over the composition range, enabling an optimum to be chosen for a given application. In this

[4] Author to whom any correspondence should be addressed.

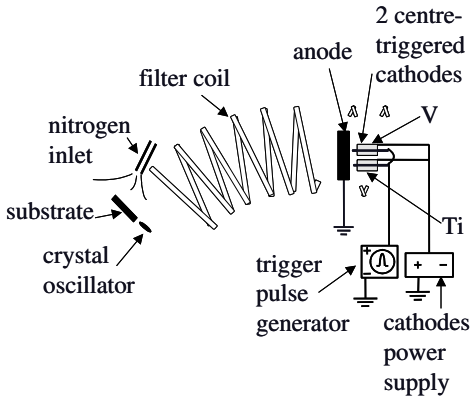

Figure 1. A schematic diagram of the two cathode pulsed cathodic arc after Gan *et al* [5].

paper we investigate the TiN/VN alloy system and use it to study the correlation between hardness, microstructure and stress. The detailed mechanical properties of these alloys will be published elsewhere [3].

Knotek and co-workers [4] prepared three compositions of the alloy TiN/VN using dc cathodic arc deposition from metallic targets of Ti/V alloys. The authors reported that the alloy prepared from the target containing 25% V in a Ti/V metal alloy showed the best wear resistance in a pin-on-disc test and the highest Vickers microhardness. In this work, we use a dual pulsed cathodic arc with two independent cathodes of the pure metals to deposit six TiN/VN films with a range of compositions as well as pure TiN and VN films. The Ti to V ratio was varied by changing the ratio of pulses delivered to each target rather than by preparing a new target for each composition as was done by Knotek and co-workers [4]. This enables us to prepare a wider range of compositions.

The pulsed cathodic arc used in this work has a centre trigger [5] which has been shown to produce a constant amount of ablation per pulse, and hence has the ability to produce controllable deposition rates. The cathodic arc produces a highly ionized plasma in which the ions have a drift velocity corresponding to an energy approximately in the range 20–80 eV [6]. These energies produce compressive stress in coatings which is known to be strongly correlated with preferred orientation [7–10]. For this reason we include a study of compressive stress in this work for a range of compositions. The microstructure of the films was investigated using cross-sectional transmission electron microscopy (X-TEM) to provide information concerning the crystallography, preferred orientation and compositional variations.

2. Experimental details

The dual source pulsed cathodic arc system is shown in figure 1 and has been described in detail previously [5]. TiN/VN alloy films were deposited using two 10 mm diameter cathodes, one each of Ti and V, separated by 20 mm centre to centre distance. The plasma from both cathodes enters the same curved magnetic field generated by a coil of 6 mm copper tubing with 28 turns, carrying a current of 40 A. A tungsten trigger wire, 0.7 mm in diameter, was located centrally in each cathode 2 mm above the cathode surface. A pulse length of 0.5 ms and a frequency of 4.5 Hz were used. The arc current applied was 220 A.

Each cathode was alternately triggered to deliver a preset number of pulses in each cycle, designed to deliver the desired composition. Table 1 gives details of the samples produced,

Table 1. EDS and EELS measurements of alloy compositions compared with calculated compositions from deposition rates.

Calculated composition of alloy	Colour	No. pulses Ti/V	Film thickness by TEM (nm) error ±2 nm	%VN calculated	% VN EDS error ±5%	% VN EELS error ±5%
TiN	Dark yellow gold	—	—	0	—	—
$Ti_{0.87}V_{0.13}N$	Dark pink gold	50/10	61	12.9	13.3	13.8
$Ti_{0.84}V_{0.16}N$	Yellow gold	51/13	76	15.9	18.0	—
$Ti_{0.77}V_{0.23}N$	Yellow gold	50/20	59	22.8	24.2	21.2
$Ti_{0.63}V_{0.37}N$	Slightly pink pale gold	30/24	69	37.2	36.0	38.7
$Ti_{0.43}V_{0.57}N$	Pale gold	44/78	68	56.8	52.0	58.4
$Ti_{0.22}V_{0.78}N$	Pale gold	16/78	63	78.3	78.8	77.4
VN	Pale gold	—	58	100	—	—

including the number of pulses in each cycle. The films are expected to have a homogeneous rather than a multilayer microstructure since each layer of metal nitride was only 0.05 nm thick, much less than a monolayer. Local melting following each ion impact should ensure that the mixing of the two metal nitrides is complete.

The system base pressure was 1×10^{-5} Torr (1.3×10^{-3} Pa). The nitrogen gas flow rate was fixed at 50 sccm and the chamber pressure was 6×10^{-4} Torr (0.08 Pa) during deposition. The *in situ* film thickness was monitored using a Maxtek MDC-360 crystal oscillator.

Square pieces of silicon wafer, 20 mm each side, nominally 330 μm thick, were used as substrates. The substrates were cleaned by ultrasonic washing in successive chemicals of hexane, acetone, ethanol, and finally deionized water. During deposition the substrates were isolated from the earthed metal holder by a glass slide, 2 mm thick. Silver conductive paint spots were used to mask the substrate to verify the film thickness *ex situ* using a Tencor P10 profilometer.

The intrinsic stress in the film was calculated from radius of curvature measurements obtained before and after deposition in two orthogonal directions using a surface profilometer. The intrinsic stress σ_f (in GPa) is given by Stoney's equation [11]:

$$\sigma_f = \frac{E_s}{6(1-\nu_s)} \frac{t_s^2}{t_f} \left(\frac{1}{R} - \frac{1}{R_b} \right) \tag{1}$$

where E_s is Young's modulus for the Si(100) wafer (125 GPa), ν_s is Poisson's ratio for the Si substrate (0.28), t_s is the thickness of the substrate, t_f is the thickness of the film (using Tencor measurements), R is the radius of the curvature of the film on substrate, and R_b is the radius of curvature of the bare substrate.

The indentation hardness was measured on the same silicon substrates using an Ultra Micro Indentation System (UMIS 2000, CSIRO, Australia), configured with a Berkovich (three-sided pyramid) diamond tipped indenter. Measurements of the load and depth penetration were recorded simultaneously using a load–partial-unload procedure [12]. Peak contact loads, P, of 0.5, 1 and 2 mN were used with the maximum indenter penetration varying from ≈20% (for $P = 0.5$ mN) to ≈60% (for $P = 2$ mN) of the film thickness. A minimum of five indents at each load was made and the results averaged. The hardness H (in GPa) was determined from:

$$H = P/A \tag{2}$$

where $A = \pi a^2$, and a is the contact radius $\left(a = \sqrt{2Rh_p - h_p^2}\right)$ in metres, with R the tip radius and h_p the plastic penetration depth. The indenter tip was calibrated using fused silica glass

(elastic modulus $E = 70$ GPa and Poisson's ratio $\nu = 0.2$) at numerous loads to determine an effective tip radius profile over a range of penetration depths.

In order to minimize the influence from the substrate, the hardness values reported here are for an indentation depth of less than about 25% of the film thickness. Further details of the hardness measurements are reported elsewhere [3].

The composition over the entire film thickness was measured using EDS performed on a Philips SEM 505 operating at 10 kV. Measurements were averaged over three positions on each sample. X-TEM was performed on a JEOL 2010 microscope equipped with a Gatan imaging filter (GIF) operating at 200 kV. The samples were prepared by tripod polishing and then ion beam thinning. Selected area diffraction (SAD) patterns were obtained, using a 100 nm diameter aperture, to study the internal microstructure of the coatings. The composition was also measured from the X-TEM samples using electron energy loss spectroscopy (EELS). The subtle colour differences reported in table 1 were observed by eye under fluorescent light.

3. Results and discussion

3.1. Film composition

Table 1 compares the composition of each film calculated from the deposition pulse ratios of both TiN and VN per cycle with that measured using EDS and EELS. The calculated values are in excellent agreement with the measured values. This result shows that our dual source pulsed deposition system can be used to prepare $Ti_{1-x}V_xN$ films with a range of compositions in a controlled manner. Subtle variations in colour were observed from a dark yellow gold (TiN) to a pale gold (VN). The thicknesses measured by TEM are also shown in table 1.

3.2. Film stress and indentation hardness

Figure 2 shows the stress and hardness as a function of x in the $Ti_{1-x}V_xN$ alloy, using the as-calculated values for composition. The hardness data point for 0.16 V was not measured. The data show a clear maximum in both stress and hardness at the same composition ($Ti_{0.77}V_{0.23}N$). The stress observed in a thin film is the net value resulting from the competition between generation and relief processes. Compressive stress is generated by energetic ion impacts and has been observed to depend on the ion energy [13, 14]. The energy of ions incident on the substrate depends on the natural energy of the ions from the cathodic arc as well as on the charge state distribution. The charge state affects the energy because of potential differences between the substrate surface and the plasma. Both the ion energies and the charge state distributions are similar for Ti and V ions [6], so it is expected that the ion energies at the substrate are similar for both metals. The stress generation process is therefore expected to be similar for all compositions of the alloy. The variation in the stress levels observed must therefore arise from the stress relief process. The relief process is strongly determined by the ease with which the material flows (i.e. the yield stress). The yield stress, σ_y, is related to the indentation hardness, H, by the formula [15]:

$$H \approx 3\sigma_y. \tag{3}$$

We propose the yield stress as the reason for the correlation between the observed stress and the indentation hardness. The correlation provides evidence that the alloy composition containing approximately $Ti_{0.77}V_{0.23}N$ has the highest yield stress. The films with lower hardness and therefore lower yield stress sustain a lower residual compressive stress, as observed in figure 2. The yield stress of a material depends on the behaviour of dislocations which in turn depends on the bonding and chemical structure of the alloy. The reason for

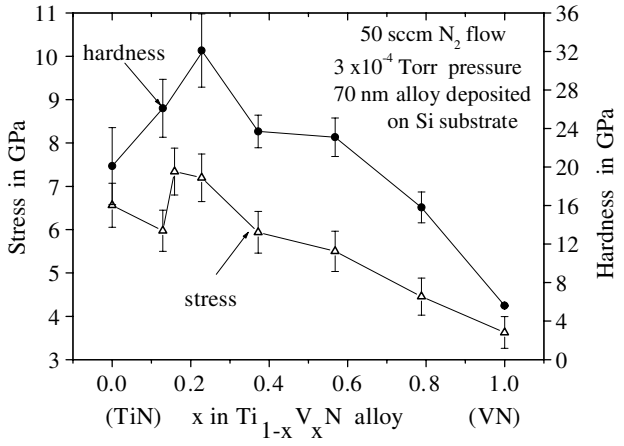

Figure 2. The stress and hardness of $Ti_{1-x}V_xN$ alloy films as a function of x. The x values were obtained using the calculated composition alloy in table 1.

the maximum yield stress at the observed composition may be the result of the pinning of dislocations. The $Ti_{0.77}V_{0.23}N$ composition is close to the 25% V content that was found by Knotek and co-workers [4] to have the highest Vickers microhardness. This is significant since the films prepared by Knotek and co-workers were much thicker than those used in this study, with thicknesses in the range 3–7 μm, suitable for Vickers hardness determination.

In contrast to the behaviour of the indentation hardness, the lattice parameter of the Ti–V–N alloy decreases linearly as the V content increases, obeying Vegard's law, as expected for simple mixing in the rocksalt structure [16–18]. The atomic radius of V (0.1346 nm) is smaller than the atomic radius of Ti (0.146 nm) [19], and therefore V substitution for Ti reduces the lattice parameter.

3.3. Microstructure

X-TEM images for several of the $Ti_{1-x}V_xN$ are shown in figure 3. In each image the film lies vertically with the surface to the left. The parallel lines are Moiré fringes which indicate two crystals of the same orientation overlapping. Selected area diffraction patterns for each film show the polycrystalline nature of the microstructure, indicated by the combination of rings and spots. In each film, the diffraction patterns can be indexed to the TiN rocksalt structure. The films did not show any strongly preferred orientation until the content of vanadium reached $x = 0.78$ (figure 3(e)), in which case it exhibited (200) orientation. This preferred orientation is indicated by the intensity of the (200) diffraction spots along a line perpendicular to the surface. The diffraction pattern for the VN (figure 3(f)) film also showed strongly preferred orientation with (200) planes aligned parallel to the surface. This type of preferred orientation has also been observed in TiN under similar low stress conditions.

Figure 4 shows energy filtered elemental maps for the $Ti_{0.87}V_{0.13}N$ sample with a resolution of approximately 1 nm. The result shows that the composition is homogeneous to this resolution throughout the cross-section of the film. The Ti^{2+} ions of 23 eV and Ti^{+} ions of 34 eV [20] are expected to penetrate to a depth of approximately 0.3 nm according to calculations using SRIM 2003 [21], which has a 5% error. Since each titanium layer is expected to be less than 0.05 nm thick, the alloy can be considered to be homogeneously mixed.

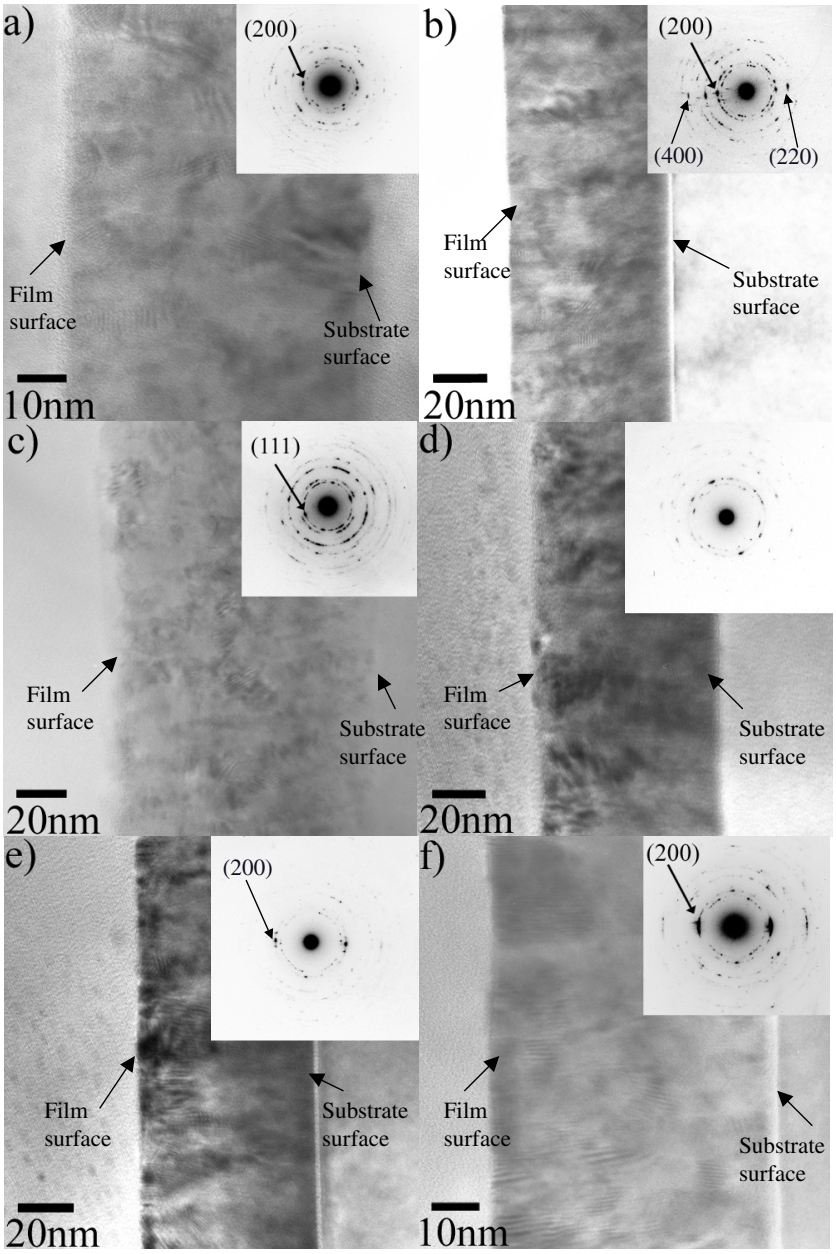

Figure 3. The TEM images and SAD patterns for (a) $Ti_{0.87}V_{0.13}N$, (b) $Ti_{0.77}V_{0.23}N$, (c) $Ti_{0.63}V_{0.37}N$, (d) $Ti_{0.43}V_{0.57}N$, (e) $Ti_{0.22}V_{0.78}N$ and (f) pure VN. Film surface on the left side of the images as shown; SAD patterns are correctly aligned with the film direction.

4. Conclusions

We show that we can synthesize homogeneous TiN/VN alloy films of any chosen composition using the pulsed cathodic arc with two pure metal cathodes and alternately triggering each cathode for a preset number of pulses. We have found that the composition $Ti_{0.77}V_{0.23}N$

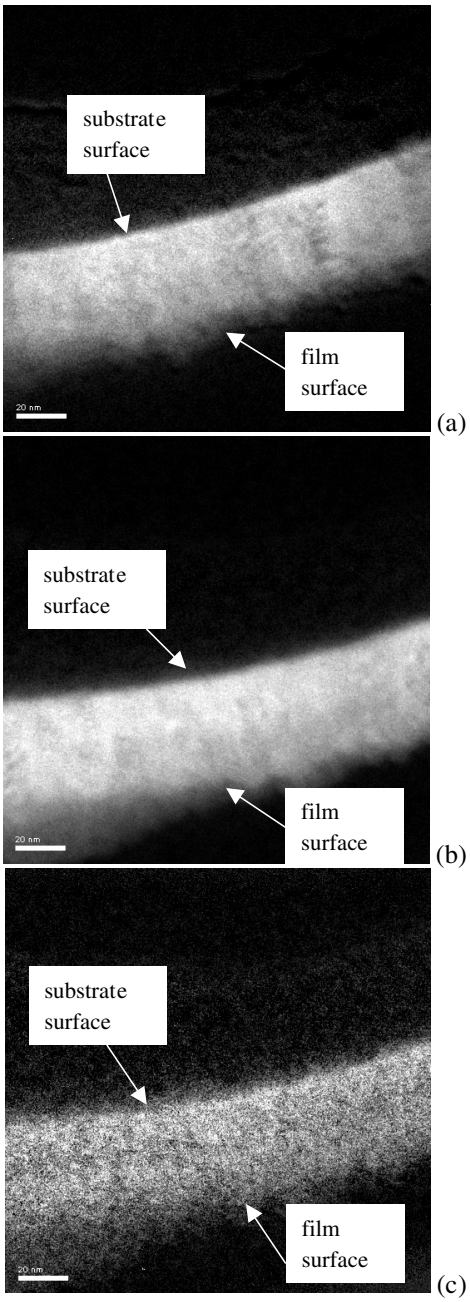

Figure 4. The EFTEM maps taken of the cross-section of the alloy $Ti_{0.87}V_{0.13}N$, showing the homogeneity of (a) nitrogen, (b) titanium and (c) vanadium content in the sample. Scale bars are 20 nm. Note that the substrate is above the film, as shown.

provides the highest yield stress in the alloy series. This composition was also found to exhibit the highest compressive stress, which we explain as a consequence of its optimum yield stress. Films with the highest vanadium content, $Ti_{0.22}V_{0.78}N$ and VN, show a preference for (200)

orientation. This work shows that the composition $Ti_{0.77}V_{0.23}N$ has a substantially higher hardness than TiN and may have an application as a high performance alloy.

Acknowledgments

We would like to thank the staff at The University of Technology, Sydney, especially Geoff McCredie for valuable technical help. This work was supported by the Australian Research Council.

References

[1] Sanjines R, Wiemer C, Hones P and Levy F 1998 *J. Appl. Phys.* **83** 1396
[2] Holleck H 1984 *Binäre und Ternäre Carbid- und Nitridsysteme der Ubergangsmetalle* (Berlin Stuttgar: Gebrüdr Bornträger) (in German)
[3] Latella B A, Gan B K, Davies K E, McKenzie D R and McCulloch D G 2004 *Surf. Coat. Technol.* at press
[4] Knotek O, Burgmer W and Stoessel C 1992 *Surf. Coat. Technol.* **54/55** 249
[5] Gan B K, Bilek M M M, McKenzie D R, Swift P D and McCredie G 2003 *Plasma Sources Sci. Technol.* **12** 508
[6] Anders A and Yushkov G Y 2002 *J. Appl. Phys.* **91** 4824
[7] Lim S H N, McCulloch D G, Bilek M M M and McKenzie D R 2003 *Surf. Coat. Technol.* **174/175** 76
[8] Gan B K, Bilek M M M, McKenzie D R, Yang S, Tompsett D A, Taylor M B and McCulloch D G 2004 *J. Phys.: Condens. Matter* **16** 1751
[9] Gan B K, Bilek M M M, McKenzie D R, Taylor M B and McCulloch D G 2004 *J. Appl. Phys.* **95** 2130
[10] Pelleg J, Zenin L Z, Lungo S and Croitoru N 1991 *Thin Solid Films* **197** 117
[11] Stoney G G 1909 *Proc. R. Soc.* A **82** 172
[12] Field J S and Swain M V 1993 *J. Mater. Res.* **8** 297
[13] McKenzie D 1993 *J. Vac. Sci. Technol.* B **11** 1928
[14] Ljungcrantz H, Hultman L, Sundgren J-E, Johansson S, Kristensen N, Schweitz J-A and Shute C J 1993 *J. Vac. Sci. Technol.* A **11** 543
[15] Ashby M F and Jones D R H 1996 *Engineering Materials 1: an Introduction to Their Properties and Applications* 2nd edn (Oxford: Pergamon) p 113
[16] Sanjines R, Wiemer C, Hones P and Levy F 1998 *J. Appl. Phys.* **83** 1396
[17] Konig U 1987 *Surf. Coat. Technol.* **33** 91
[18] Knotek O, Barimani A, Bosserhoff B and Löffler F 1990 *Thin Solid Films* **193** 557
[19] Alcock N W 1990 *Bonding and Structure: Structural Principles in Inorganic and Organic Chemistry* (New York: Ellis Horwood)
[20] Bilek M M M, Martin P J and McKenzie D R 1998 *J. Appl. Phys.* **83** 2965
[21] Ziegler J F, Biersack J P and Littmark U 1984 *The Stopping and Range of Ions in Solids* (*Stopping and Ranges of Ions in Matter* vol 1) (New York: Pergamon)